Pulmonary response prediction through personalized basis functions in a virtual patient model

Computer Methods and Programs in Biomedicine 244 (2024) 107988

Contents lists available at ScienceDirect

Computer Methods and Programs in Biomedicine

journal homepage: www.elsevier.com/locate/cmpb

Pulmonary response prediction through personalized basis functions in a virtual patient model

Trudy Caljé-van der Klei [a,*], Qianhui Sun [a,b], J. Geoffrey Chase [a], Cong Zhou [a], Merryn H. Tawhai [c], Jennifer L. Knopp [a], Knut Möller [d], Serge J. Heines [e], Dennis C. Bergmans [e], Geoffrey M. Shaw [f]

[a] Department of Mechanical Engineering, Centre for Bio-Engineering, University of Canterbury, Christchurch, New Zealand
[b] University of Liége, Liége, Belgium
[c] Auckland Bioengineering Institute, The University of Auckland, Auckland, New Zealand
[d] Institute for Technical Medicine, Furtwangen University, Villingen-Schwenningen, Germany
[e] Department of Intensive Care, School of Medicine, Maastricht University, Maastricht, Netherlands
[f] Department of Intensive Care, Christchurch Hospital, Christchurch, New Zealand

ARTICLE INFO

Keywords:
Virtual patient
Digital twin
Mechanical ventilation
Critical care
Basis function
Prediction
Elastance
Dynamic functional residual capacity
Lung distension
VILI
Pressure-volume loop

ABSTRACT

Background and Objective: Recruitment maneuvers with subsequent positive-end-expiratory-pressure (PEEP) have proven effective in recruiting lung volume and preventing alveoli collapse. However, determining a safe, effective, and patient-specific PEEP is not standardized, and this more optimal PEEP level evolves with patient condition, requiring personalised monitoring and care approaches to maintain optimal ventilation settings.
Methods: This research examines 3 physiologically relevant basis function sets (exponential, parabolic, cumulative) to enable better prediction of elastance evolution for a virtual patient or digital twin model of MV lung mechanics, including novel elements to model and predict distension elastance. Prediction accuracy and robustness are validated against recruitment maneuver data from 18 volume-controlled ventilation (VCV) patients at 7 different baseline PEEP levels (0 to 12 cmH_2O) and 14 pressure-controlled ventilation (PCV) patients at 4 different baseline PEEP levels (6 to 12 cmH_2O), yielding 623 and 294 prediction cases, respectively. Predictions were made up to 12 cmH_2O of added PEEP ahead, covering 6 × 2 cmH_2O PEEP steps.
Results: The 3 basis function sets yield median absolute peak inspiratory pressure (PIP) prediction error of 1.63 cmH_2O for VCV patients, and median peak inspiratory volume (PIV) prediction error of 0.028 L for PCV patients. The exponential basis function set yields a better trade-off of overall performance across VCV and PCV prediction than parabolic and cumulative basis function sets from other studies. Comparing predicted and clinically measured distension prediction in VCV demonstrated consistent, robust high accuracy with $R^2 = 0.90–0.95$.
Conclusions: The results demonstrate recruitment mechanics are best captured by an exponential basis function across different mechanical ventilation modes, matching physiological expectations, and accurately capture, for the first time, distension mechanics to within 5–10 % accuracy. Enabling the risk of lung injury to be predicted before changing ventilator settings. The overall outcomes significantly extend and more fully validate this digital twin or virtual mechanical ventilation patient model.

1. Introduction

Protective mechanical ventilation (MV) strategies have improved intensive care unit (ICU) care by limiting tidal volumes and driving pressures [1–7]. Staircase recruitment maneuvers (RMs) followed with positive-end-expiratory-pressure (PEEP) is one common protective MV approach for acute respiratory distress syndrome (ARDS) and respiratory failure patients to keep alveoli open and improve oxygenation [2,8–12]. However, insufficient, or excessive airway pressure or tidal volume can lead to ventilator induced lung injury (VILI), increasing morbidity and mortality [10,13–25]. Accurate, predictive, and patient-specific MV strategies could significantly advance care and minimise VILI [26–28].

Utilising an accurate predictive model of lung mechanics with a

* Corresponding author.
E-mail address: trudy.calje-vanderklei@pg.canterbury.ac.nz (T. Caljé-van der Klei).

https://doi.org/10.1016/j.cmpb.2023.107988
Received 21 June 2023; Received in revised form 16 November 2023; Accepted 17 December 2023
Available online 19 December 2023

ventilated patient has significant potential in aiding clinical decisions. The predictive mechanics model would enable a safer setting of positive end expiratory pressure to minimise lung elastance and minimise the risk of over distention and ventilator induced lung injury [29]. More specifically, the elastance that is often referred to in lung mechanics is associated as that during inspiration. If the elastance is not at its optimal point, the alveolar are at risk of bursting or underinflating. In either case, oxygenation into the blood stream decreases. Optimal elastance correlates directly to the recruitable volume. If this value is set too low, the alveolar will not expand to their full potential, if set too high the alveolar are at risk of tissue damage due to overdistension. Another primary factor to be considered is selecting the optimal PEEP. This value changes the lung mechanics of a person under ventilation both by their value and shape of P-V loops. As this change is visibly different for each person, the use of prediction methods tailored to a person's lung mechanics has significant potential in aiding clinical decisions and preventing overdistension.

Currently, no effective standardised clinical method exists to determine optimal patient-specific PEEP, leading to uncertainty, variability, and increased risk [13,28,30–33]. Model-based methods are one way of personalising care [28]. While many models successfully capture lung dynamics [34–39], very few can accurately predict the pulmonary response over PEEP [26,40–42]. An accurate, predictive lung mechanics model, or virtual MV patient, would let clinicians test new MV settings without risk, enabling safer, more optimal, personalised care.

MV modes can be broadly classified as either volume-controlled ventilation (VCV) or pressure-controlled ventilation (PCV) [9,43,44]. VCV delivers a controlled flow to guarantee a targeted tidal volume but can lead to VILI if the resulting uncontrolled airway pressure is too high [45,46]. PCV sets a desired airway pressure profile and driving pressure, and the resulting tidal volume is an uncontrolled function of patient-specific lung mechanics [43,44,47]. To avoid overshoot in PCV an appropriate deceleration of input flow can be used [43,47,48]. Thus, the resulting tidal volume can be variable in PCV, increasing the risk of VILI [45,47–49].

Clinically, VCV sets peak inspiratory volume (PIV) to minimise risk of volutrauma. Similarly, PCV limits peak inspiratory pressure (PIP) to prevent barotrauma/overdistension [13,45,50]. However, no significant difference in clinical outcome between using a VCV approach or a PCV approach has been observed [43,47,49,51–53]. Hence, the choice of MV mode is primarily a function of patient synchrony and response to MV, and clinician preference [44,51].

Basis functions have been proposed as a method for targeted biomedical information simulation and prediction [26,41,42,54–64]. Well-defined, they offer additional, model-based insight into physiological mechanics and responses [26,41,59,65–69]. The ability of basis functions to model and predict lung elastance and resistance evolution was demonstrated using a linear single compartment lung model, but lacked accuracy in capturing some nonlinear lung mechanics, in both inspiration and expiration [26,55,56,66,70,71].

A nonlinear, physiologically-relevant hysteresis loop model (HLM) using basis functions accurately captured and predicted the evolution of lung mechanics as MV settings change for both VCV and PCV patients [42]. However, it did not assess if these basis functions were optimal compared to other choices. None of these approaches captured distension and its risk, which is critical to directly managing the risk of VILI.

This research extends this virtual MV patient model framework to include clinically critical, nonlinear lung distension mechanics, and assesses it across 3 basis function sets to compare performance in predicting lung mechanics in response to changes in PEEP. Performance trade-offs show which elements of these basis functions are necessary to guarantee accuracy and clinical relevance, and the inclusion of distension adds significant new clinical utility.

2. Methods

2.1. HLM lung mechanics model

The dynamic equation of motion for the HLM lung mechanics model is defined [42]:

$$M\dot{V}(t) + R\dot{V}(t) + K_e V(t) + K_{h1} V_{h1} + K_{h2} V_{h2} = f_V(t) + PEEP \tag{1}$$

Where M is the normalised mass, V is the volume of air delivered to the lungs, V_{h1} and V_{h2} are hysteretic volume response during inspiration and expiration, respectively, K_e represents the alveolar recruitment elastance (defined further in Section, Appendix A), named $k2$ in this approach to be predicted in the proposed basis functions, K_{h1} and K_{h2}, are determined by two nonlinear hysteretic springs for alveolar hysteresis elastance during inspiration and expiration, respectively. These are defined as:

$$K_{h1} = k1 - k2 \tag{2}$$

$$K_{h2} = k3 - k4 \tag{3}$$

where k1-k4 can be identified from the constructed P-V loop using the HLA approach, as shown in the example of Fig. 1. For other parameters in Eq. (1), R is the airway resistance, PEEP is the positive end-expiratory pressure, and $f_V(t)$ is the steady-state input force. The detailed formulations for calculating each parameter can be found in Online Appendix A and Zhou et al. [42].

2.2. P-V loop identification

At any initial, baseline $PEEP_i$ ($i = 1$) level, the hysteresis loop analysis method (HLA) is applied to identify elastance values for the whole breath. HLA separates the P-V loop for a breath into 5 segments, as shown in Fig. 1. For expiration, 2 segments are identified with two elastances, $k3$ and $k4$, respectively. For inspiration, the half cycle is first divided into 2 segments, with $k1$ and $k2$. Subsequently, the $k2$ segment is assessed using a statistical test to find any potentially, increased stiffness (reduced compliance) third segment, denoted $k2end$, arising from any distension. This last term, $k2end$, uses a separate basis function prediction procedure to capture possible over-distension as PEEP rises.

The lower inflection point is a critical piece defining where the analysis for $k2$begins. It is also the point that is currently used to determine the minimal level of PEEP where alveolar recruitment begins. Examples are shown in Fig. 1 for VCV and PCV clinical PV loops constructed from McREM and Maastricht trial data, respectively.

2.3. Basis function sets for elastance prediction

Using the same HLA identification procedure, three (3) physiologically relevant sets of basis function for predicting the evolution of recruitment elastance at higher PEEP levels ($k2_i, i > 1$) are examined as a function of the $k1$, $k2_1$, $k2end_1$, $k3$, $k4$ values identified using HLA from measured PV loop clinical data at a baseline PEEP ($i = 1$). Exponential (EXP) basis functions have been used in prior studies to estimate pulmonary elastance evolution [42,55,57], while basis parabolic (PARA) functions have also shown promise [26,41,63]. The third cumulative (CUMU) basis function set was developed and validated in prior work [64] and are also examined here with minor modification to suit the HLM model. The evolution and prediction of distension at higher PEEP levels ($k2end_i, i > 1$) is developed in prior work [72] and kept the same for all three basis function sets.

These three basis functions have been chosen as they include nonlinear recruitable response and linear distension response which are all physiologically relevant to the analysis of lung mechanics, specifically volume changes. There are a variety of other basis functions that are applicable for this analysis, however, these three represent some

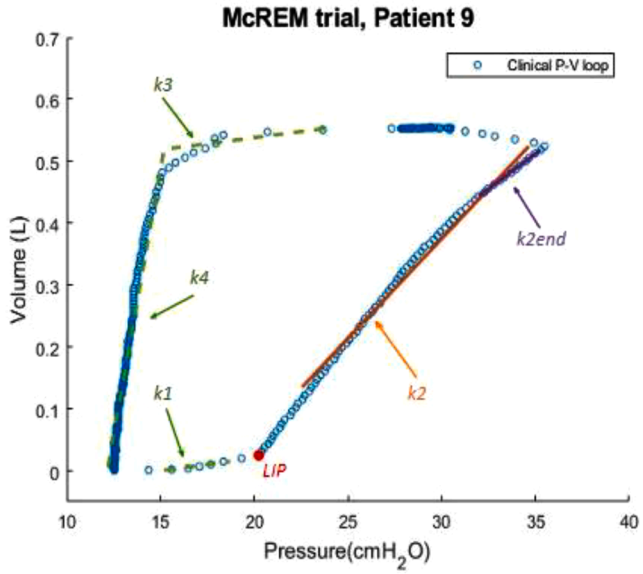

(a) the McREM trial (VCV mode) – typical distension

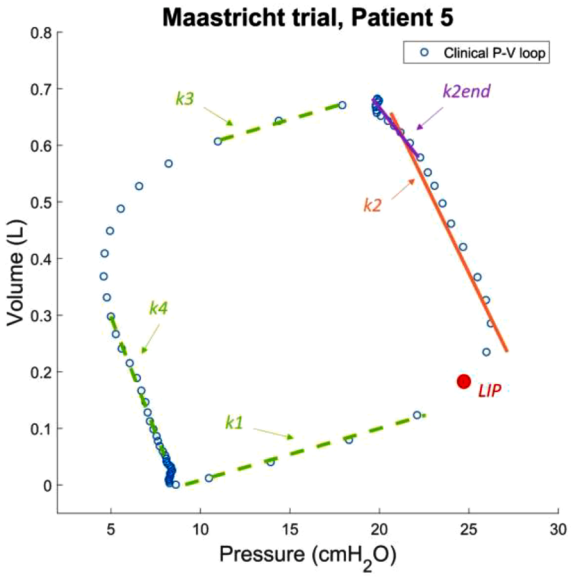

(b) the Maastricht trial (PCV mode) – typical distension

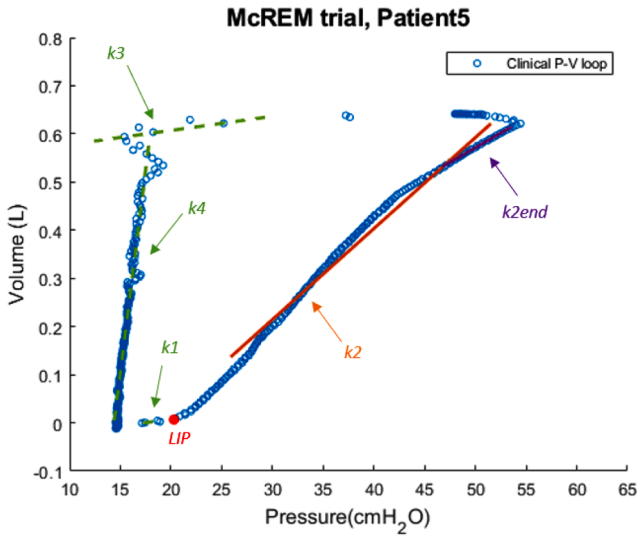

(c) the McREM trial (VCV mode) – extreme distension

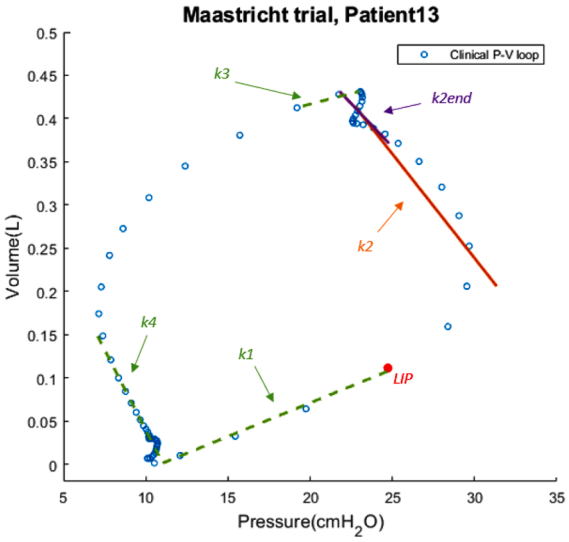

(d) the Maastricht trial (PCV mode) – extreme distension

Fig. 1. Examples of HLA identification for measured clinical P-V loops, showing both typical distension and extreme distension cases. (a) the McREM VCV trial (typical distension), Patient 9 at PEEP = 12 cmH_2O and showing the lower inflection point (LIP); (b) the Maastricht PCV trial (typical distension), Patient 5 at PEEP = 8 cmH_2O, where k2end is negative sloped due to the adaptive tube compensation used in this PCV trial; (c) the MCREM VCV trial (extreme distension), Patient 5 at PEEP = 14 cmH_2O and showing LIP; and (d) the Maastricht PCV trial (extreme distension), Patient 13 at PEEP = 10 cmH_2O.

clearly distinct and previously proven properties within this model framework.

2.3.1. *Exponential basis function set – EXP*

The exponential basis function set assumes elastance has a bowl shape across PEEP levels, and is the same as previously presented [42]:

$$k2_i = \left(\frac{PEEP_i}{k1} + \frac{k2_1}{k1} * e^{b*\frac{PEEP_i}{k1}}\right) * k1 \tag{4}$$

$$b = \frac{k1}{PEEP_1} * \log\frac{k2_1 - PEEP_1}{k2_1} \tag{5}$$

Where b is the exponential rate of recruitment, all other terms are as previously defined, and $PEEP_i$ is the predicted PEEP level.

2.3.2. *Parabolic basis function set – PARA*

The parabolic basis function set is derived from the proven functions in [26] with similar, but different overall shape as the EXP set, and re-derived in terms of $PEEP_i$ and the other baseline PEEP identified inputs for use in this analysis [63]:

$$k2_i = \left(\frac{PEEP_i}{k1 * \beta1} + \beta2 * \left(\beta1 - \frac{PEEP_i}{k1}\right)^2\right) * k1 \tag{6}$$

$$\beta1 = 2 - \frac{\widehat{k1}}{k1} \tag{7}$$

$$\beta 2 = \frac{\frac{k2_1}{k1} - \frac{PEEP_1}{k1 * \beta 1}}{\left(\beta 1 - \frac{PEEP_1}{k1}\right)^2} \tag{8}$$

Where all terms are previously defined or given here, and $PEEP_i$ is the prediction PEEP level. $\widehat{k1}$ is the average value of alveolar elastance for first inspiration segment, estimated with value 130 over both VCV and PCV datasets [42].

2.3.3. Cumulative basis function set – CUMU [64]

The cumulative basis function set models the evolution of elastance as continuously increasing at a combination of all the predicted PEEP levels, and is defined [63]:

$$k2_i = \left(\frac{\delta 1}{k1} * \sum_{j=2}^{j=i} \Phi_j + \delta 2 * PEEP_1 * \sum_{j=2}^{j=2} \Phi_j * \sum_{j=2}^{j=3} \Phi_j * \ldots * \sum_{j=2}^{j=i} \Phi_j\right) * k1 \tag{9}$$

$$\delta 1 = \left(\frac{k2_1}{k1} - \frac{PEEP_1}{k1 - k2_1}\right) * k1 \tag{10}$$

$$\delta 2 = \frac{1}{k1 - k2_1} \tag{11}$$

$$\Phi_i = \begin{cases} \left(1 + PIP_{fit_{error}}\right)^{-1} & , \ i = 2 \\ \vartheta_1 * \left(PEEP_i - PEEP_{i-1}\right) & , \ i > 2 \end{cases} \tag{12}$$

Where $\vartheta_1 = 0.0087$ and $PIP_{fit_{error}} = \frac{fitted\ PIP - clinical\ PIP}{clinical\ PIP}$ at baseline $PEEP_1$. The value assigned to ϑ_1 is derived using an optimization method by determining the local minima/maxima [73]. Since the highest PEEP level studied is lower than or equal to $PEEP_{max}$=24 cmH_2O, basing on prior work [64], the value of Φ_i when $PEEP_i > PEEP_{max}$ is not presented.

2.3.4. Basis function sets summary

Fig. 2 shows an example of the basis function terms changing over PEEP for all 3 basis function sets, where $k2_1 = 30$ cmH_2O/L, $k1 = 80$c mH_2O/L, $PEEP_1 = 2$ cmH_2O and $PIP_{fit_{error}} = -1/35$. The goal is to delineate how each term in Eqs. (4), (6), and (9) for each basis function set, models elastance evolution. The EXP set captures exponentially falling elastance with increased recruitment combined with rising elastance due to possible distension or increasing lung filling as pressures rise. It is thus physiologically relevant and readily explicable. The PARA set is similar to EXP set in shape and assumptions, but showed improvements in limited prior studies with a simpler single compartment lung mechanics model [26]. Finally, the CUMU set views net, overall, all-cause lung elastance as always rising as a function of PEEP, while the patient-specific rate of increase is related to patient-specific identified $k1$ and $k2$ values identified at baseline PEEP using HLA.

2.4. Distension prediction (k_2end)

In addition, for all three basis function sets, $k2end$ captures the potential over-distention at the end of inspiration, which is clinically relevant as it indicates potential overdistension due to excessive pressure and VILI [13] and is proved to be effective in improving PIP predictions [72]. Then, in this approach, $k2end$ prediction function remains the same as prior approach and for all 3 basis function sets:

$$k2end_i = \left(\frac{PEEP_i}{k2_i} + \frac{k2end_1}{k2_1} * \left(\theta 1 + \left(\Delta PEEP * \theta 2\right)^2\right)\right) * k2_i \tag{13}$$

$$\theta 1 = \frac{k2end_1 - PEEP_1}{k2end_1} \tag{14}$$

$$\theta 2 = \frac{EELV_1}{PIV_1 - EELV_1} \tag{15}$$

Where $EELV_1$ is end expiratory volume and PIV_1 is peak inspiratory volume identified at baseline PEEP.

2.5. Overall identification and prediction procedure

The overall identification and prediction procedure flowchart is shown in Fig. 3. This method is outlined further in [42], including the extension of the original HLA method for both the LIP predictions in PCV and VCV modes. The method used for determining the value of distension, $k2end$, differs depending on the mode of ventilation. For the PCV mode, $k2end$ is held constant for the given breath under evaluation as determined from the identification stage. Contrarily, $k2end$ is predicted at each evaluated breath for the VCV mode. This method is outlined further in [74].

Therefore, the ability to accurately predict any distension and the PIV or PIP is critical to avoiding unintended injury. The ability to also predict, with these values, the elastance level at each PEEP (k2) means we can minimise work of breathing and set PEEP to minimum elastance, while, as above, avoiding lung injury and over distension. These methods have been researched in prior work [7,75].

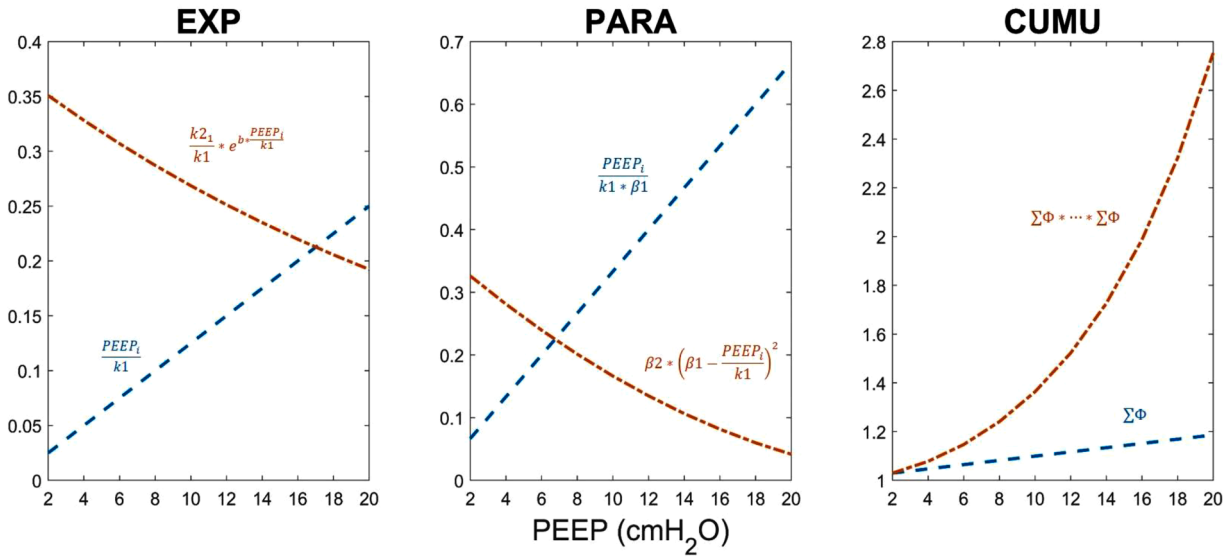

Fig. 2. Illustration of the contribution of each term and how they change over PEEP for all 3 basis function sets in Eqs. (4)–(12).

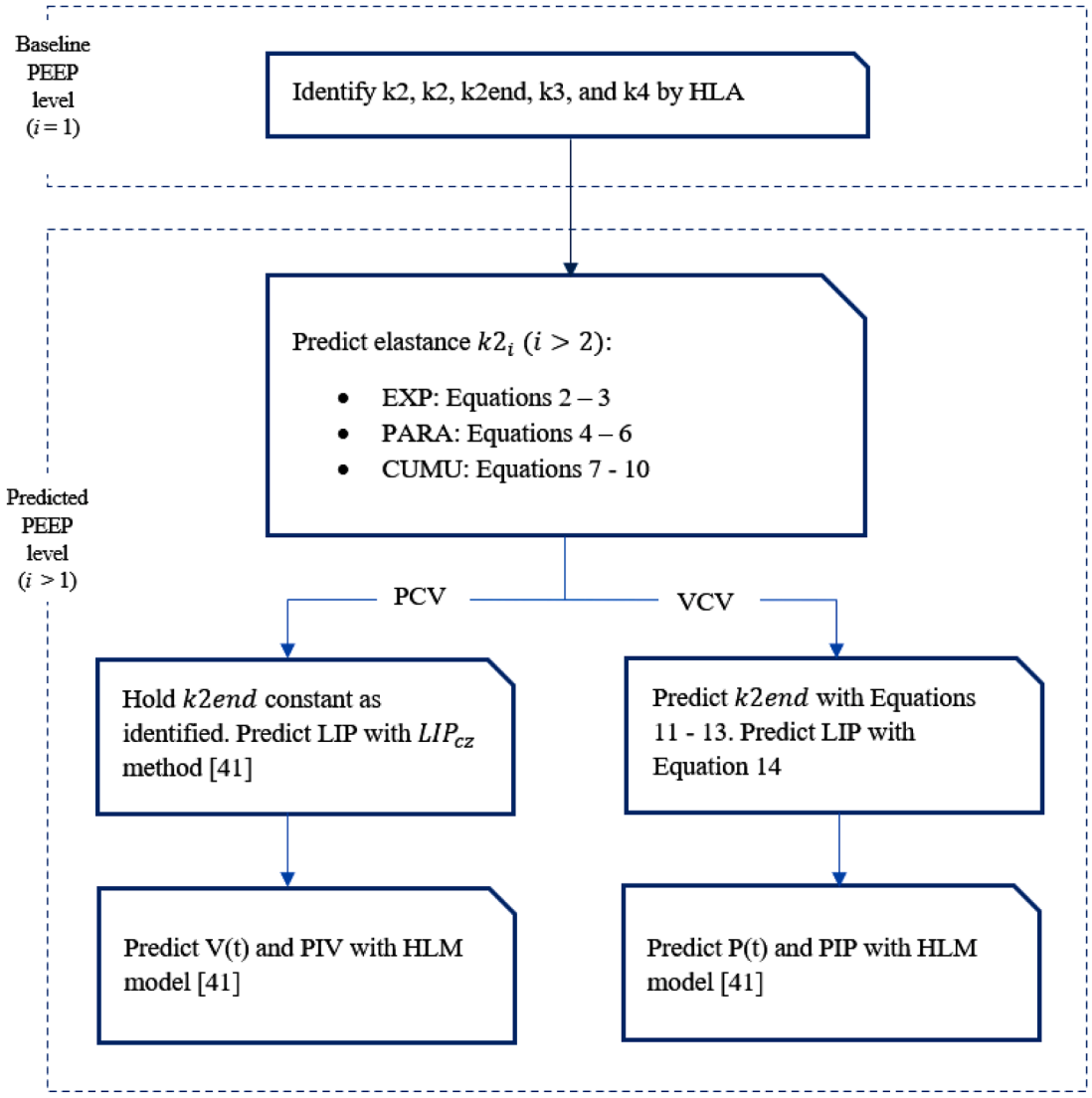

Fig. 3. Flowchart of the overall identification ($i = 1$) and prediction ($i > 1$) procedure.

In this research we are predicting the most likely value for each parameter. We use R-squared (R2) as a metric to define these predictions in quantitative way for comparison. the most value R2 are those for predictions 2 and 4 cmH_2O ahead. These are the clinically relevant scenarios and where this modelling could assist clinicians.

2.6. Patient data

Pressure and flow data from 32 ventilated patients in the ICU (18 from the McREM trial [76] and 14 from Maastricht trial) were used to validate the three (3) proposed basis function sets in this study.

2.6.1. VCV trial

In the McREM trial, all 18 patients were fully sedated and intubated under invasive volume-controlled ventilation, with tidal volume set to 8 ± 2 ml/kg based on ideal body weight [76]. The McREM trial was conducted across eight German university ICUs from September 2000 to February 2002. All 18 patients were ventilated with a Draeger Evita 4 ventilator. During ventilation, an end-inspiratory hold of 0.2 s is applied for each breath and data were sampled at 125 Hz. Patient demographics are in Table 1

One increasing staircase RM with 2 cmH_2O step was performed for each patient starting at 0 cmH_2O. The prediction procedure is applied for further higher PEEP levels ($i = 2, \ldots, 7$) after identification at baseline PEEP ($i = 1$). To test the robustness and generality of HLM model and basis function sets, prediction tests are applied across a range of baseline PEEP = 0, 2, 4, 6, 8, 10, and 12 cmH_2O with a further 6 prediction steps (2 cmH_2O interval) from each baseline level, yielding a maximum value for $\Delta PEEP = 2 \times 6$ steps = 12 cmH_2O. There are thus a total of 623 predictions across the 7 baseline PEEP test groups. The test group setting is shown schematically in Fig. 4.

2.6.2. PCV trial

The Maastricht trial comprised 14 patients recruited in Maastricht, Netherlands from November 2017 to February 2018 (METC 17–4–053). All patients were treated with Bi-level Positive Airway Pressure pressure-controlled ventilation with automatic tube compensation (ATC). Patient demographics are in Table 2.

One full staircase RM with increments and decrements of PEEP in 2 cmH_2O intervals was performed for each patient, where only the increasing RM arm is studied. Different from the McREM trial, RM baseline PEEP varies for all 14 patients (10 patients at 6 cmH_2O, 3 patients at 8 cmH_2O, and 1 patient at 10 cmH_2O). Thus, ???tests are applied at baseline PEEP = 6, 8, 10, and 12 cmH_2O, while prediction steps are also 6 further steps with 2 cmH_2O intervals, yielding maximum $\Delta PEEP = 2 \times 6$ steps = 12 cmH_2O. Thus, there are 294 predictions in

Table 1
VCV patients and clinical trial demographics in the McREM pilot trial [76]. TBI = Traumatic Brain Injury, SDH = Subarachnoid Hemorrhage, SAH = Subarachnoid and Subdural Hemorrhage.

Patient No	Gender	Age (years)	Length of MV (days)	PaO_2/ FiO_2 (mmHg)	Clinical Diagnostic
1	m	74	10	298	SAH, SDH
2	f	50	8	202	Pancreatitis, pneumonia
3	f	30	8	162	Peritonitis, sepsis
4	f	49	3	289	Pneumonia
5	m	34	10	192	open TBI
6	m	67	4	234	Post reanimation
7	m	39	10	188	Sigma perf., peritonitis
8	m	42	9	235	Pneumonia, pancreatitis
9	m	51	5	230	TBI, pneumonia
10	m	77	6	225	Pneumonia
11	m	37	10	163	Pneumonia
12	m	41	16	178	Peritonitis
13	m	62	2	288	SDH
14	m	39	7	143	TBI, pneumonia
15	m	74	9	271	S/P coronary artery bypass grafting, pneumonia
16	m	59	19	75	ARDS
17	m	45	8	173	Blunt abdominal trauma, pneumonia
18	m	42	11	260	Alcoholism, GI bleeding, sepsis

total across 4 baseline PEEP level test groups. The 4 test groups are analysed using the same procedure as for the McREM trial, where the first PEEP level is 6 cmH_2O in this case.

2.7. Validation and error analysis

In VCV, PIP is the critical indicator for VILI due to overdistension due to excessive pressure [13,45,50]. Similarly, in PCV, PIV reflects volutrauma risk [51,77]. Boxplots provide the PIP or PIV error distribution over all baseline PEEP levels with absolute median error noted. Correlations between clinical and model predicted PIP or PIV are plotted with R^2 values calculated for the 1:1 perfect match line to further show spread and error. In VCV patients, the value of *k2end* for PIP prediction is assessed by comparing PIP predictions with and without this term to show the error reduction achieved by accounting for distension.

2.8. Comparative variables

Elastance segment *k*2 is used to determine *k2end*, where there is increased stiffness (reduced compliance) at the end of inspiration, associated with overdistension. Poor ventilator settings can lead to overdistention, in turn leading to increased potential for barotrauma or volutrauma causing VILI. Thus, predicting *k2end* accurately is also critical to safely personalising MV care. Predicted and identified *k*2values were compared using absolute error. From this error, median errors were calculated to determine the relative performance of the basis functions.

For VCV patients, model predicted PIP values are compared to values from the McREM study. Equivalently, for PCV patients, PIV is compared to clinical values from the Maastricht study data. In both instances, signed and absolute errors were determined for each case, giving a median error at each respective baseline PEEP for the three basis function sets. These errors in combination with plotted trends assist in determining the most accurate and/or optimal basis functions for different MV modes.

3. Results

3.1. VCV patients and trial

3.1.1. Comparison of identified elastance and predicted elastance (*k2*) for VCV

The elastance prediction comparison for VCV was conducted across the same 7 different PEEP levels for each of the three basis functions (EXP, PARA and CUMU). As depicted in Fig. 5, the scatter plots observe a trend in which the identified elastance obtained from the measured data is typically higher than the predicted value. This is the case for all three basis functions. With the boxplots on the right-hand side, the PARA basis function shows the lowest errors and least bias (overall) of the three basis function sets, whereas the errors for the CUMU set are more than double that of the PARA set (median error comparison).

Table 2
PCV patients and clinical trial demographics in the Maastricht pilot trial. CABG = Coronary Artery Bypass Grafting, AVR = Aortic Valve Replacement.

Patient No	Gender	Age (years)	PaO_2/ FiO_2 (mmHg)	Clinical Diagnostic
1	Male	77	255	CABG
2	Female	85	308	CABG
3	Male	57	323	CABG
4	Male	47	233	CABG
5	Male	73	150	AVR
6	Male	75	383	CABG
7	Female	71	443	AVR
8	Male	76	398	CABG
9	Female	64	255	Subarachnoid Haemorrhage
10	Female	68	428	Pneumonia
11	Female	78	143	Pneumonia
12	Female	18	83	Mitral and Tricuspid Valve Replacement
13	Female	71	443	Pneumonia
14	Male	36	158	CABG

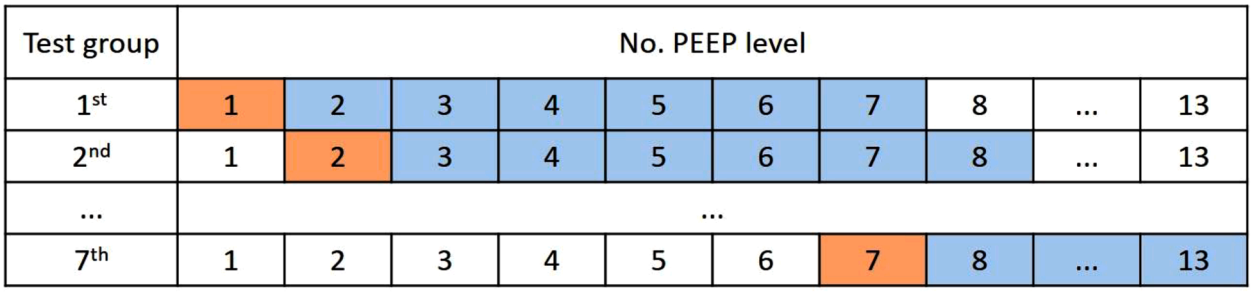

Fig. 4. Schematic test group setting for the McREM trial. Orange coloured levels present the identification baseline PEEP level, while blue coloured levels present the further 6 prediction levels used to test prediction. Intervals in 2 cmH_2O are set between each PEEP level, while first PEEP level is 0 cmH_2O by protocol. PEEP levels are numbered in these 2 cmH_2O steps [72].

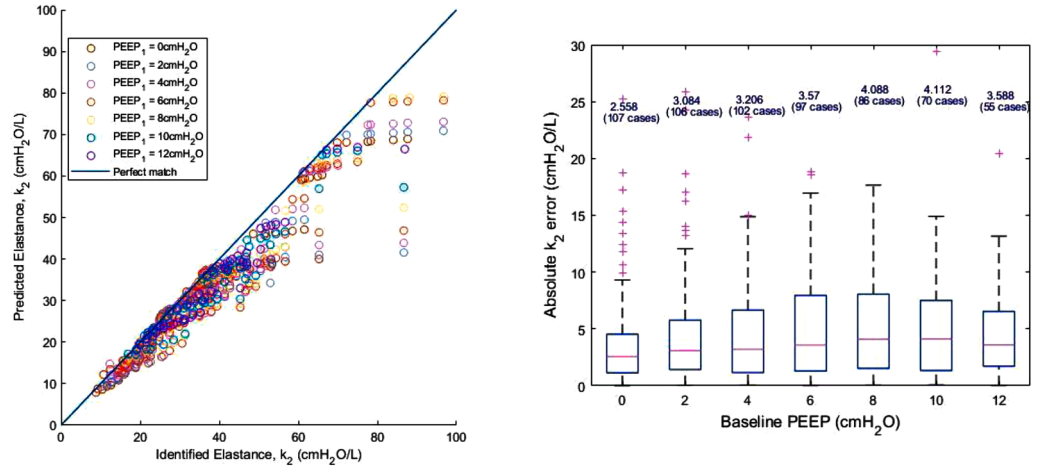

a) EXP set

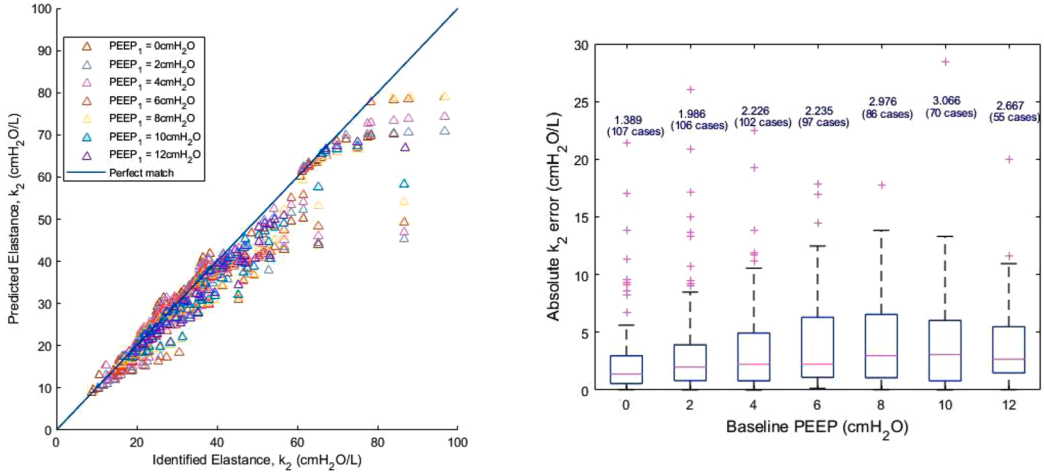

b) PARA set

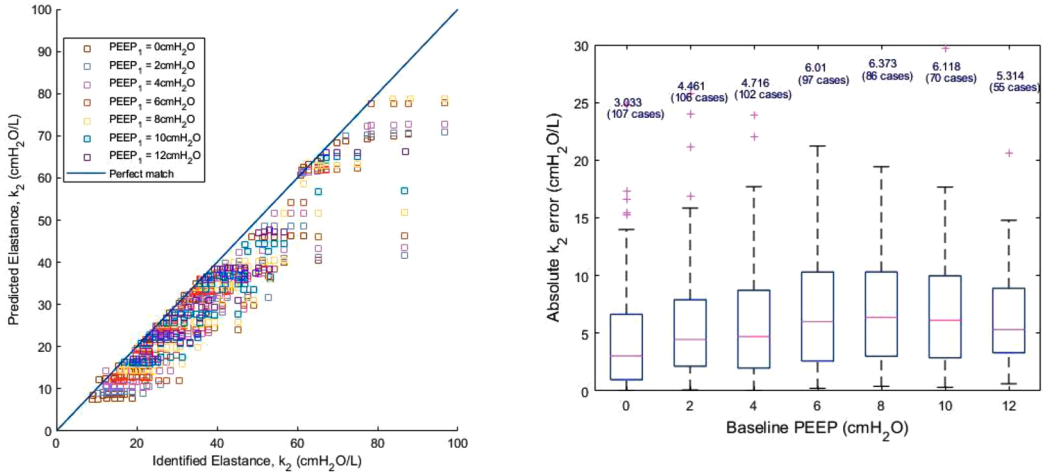

c) CUMU set

Fig. 5. Correlation plots of Predicted k_2 vs Clinical k_2 (left) and boxplots for absolute $k_2$prediction errors with noted median errors (cmH_2O/L) over 7 baseline PEEPs (right) for (a) EXP, (b) PARA, and (c) CUMU basis function sets with VCV data.

3.1.2. Peak inspiratory pressure (PIP) prediction for VCV

Boxplots of absolute PIP prediction errors across all 7 test groups (baseline PEEP = 0, 2, 4, 6, 8, 10, and 12 cmH_2O) with 6 prediction steps are shown in the right-hand side of Fig. 6, while the relationships between clinical PIP and predicted PIP are presented separately in the left-hand side of Fig. 6 for all 3 sets (623 predictions) with overall R^2 values of 0.90, 0.85, and 0.88 for the EXP, PARA, and CUMU basis function sets, respectively. Table 3 shows the R^2 values over shorter

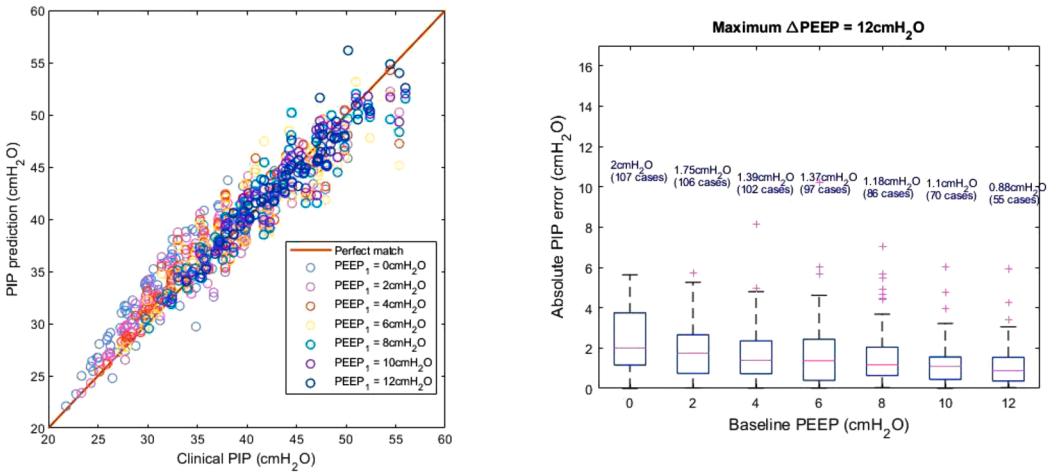

(a) EXP set

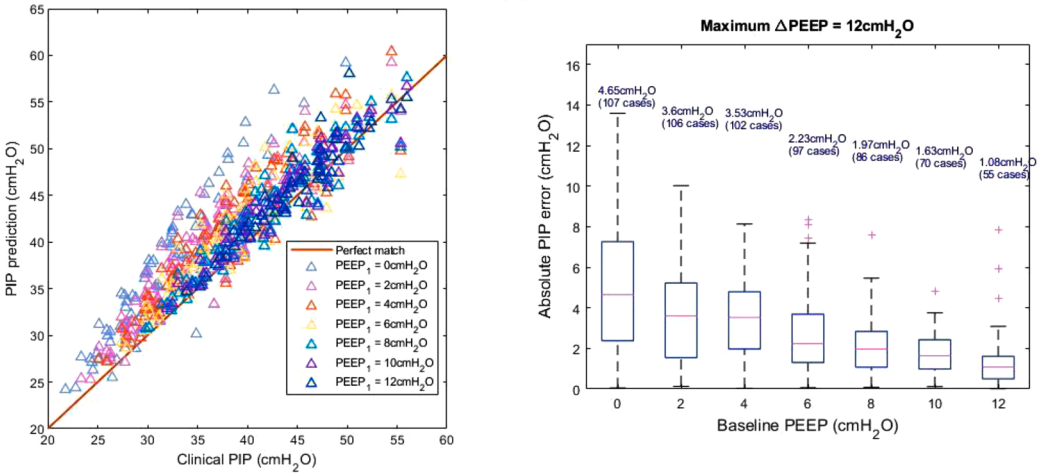

(b) PARA set

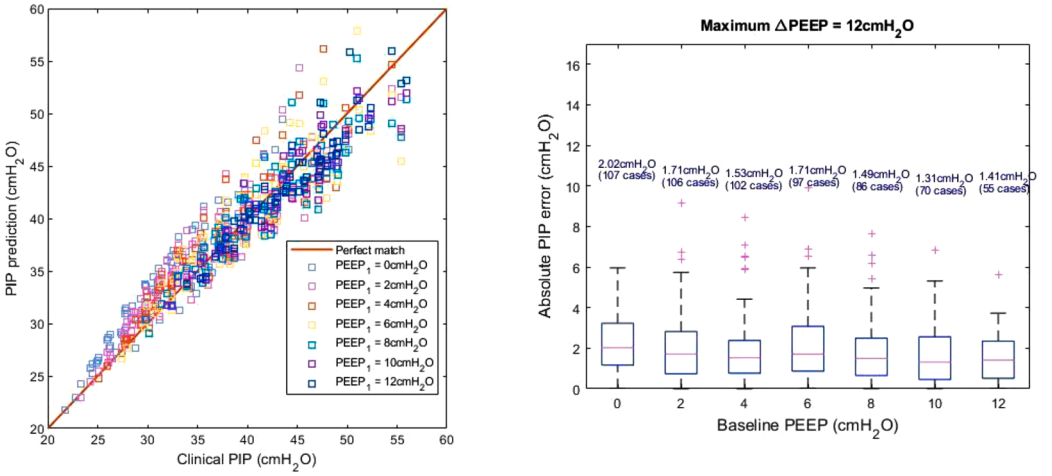

(c) CUMU set

Fig. 6. Correlation plots of Predicted PIP vs Clinical PIP (left) and boxplots for PIP prediction errors with noted median errors (cmH_2O) over 7 baseline PEEPs (right) for (a) EXP, (b) PARA, and (c) CUMU basis function sets, yielding overall $R^2 = 0.90$ in EXP, $R^2 = 0.85$ in PARA, and $R^2 = 0.88$ in CUMU among 623 prediction cases in VCV.

prediction intervals are higher, ranging from $R^2 = 0.91–0.96$ in the first three rows of the table.

Comparing basis functions, the PARA set in VCV prediction yields the 'worst' performance with higher median errors and an overall lowest R^2 value = 0.85. However, the higher median error is partly a result of bias, with 70.6 % predictions of overshooting the clinical value, which has potential clinical utility in guiding MV as it can lead to more conservative clinical decisions. Bias for the other sets are 60.8 % for EXP and 53.0 % for CUMU. EXP and CUMU yield similar overall performance in all 7 predictions, while overall 90 % of PIP prediction errors are within 3.95 cmH_2O. However, EXP tends to have a better performance than CUMU at baseline PEEP $\geq$ 6 cmH_2O, and thus is better at clinically relevant PEEP levels.

3.2. PCV patients and trial

3.2.1. Comparison of identified elastance and predicted elastance (k_2) for PCV

Fig. 7 depicts the comparison of identified elastance and predicted elastance for PCV alongside their respective error boxplots. Comparisons were conducted for each of the three basis functions across four different baseline PEEP levels (PEEP = 6, 8, 10, 12 cmH_2O). The elastance values are all negative, due to the specific geometric shape of the P-V loops for PCV, as shown in Fig. 1(b). PCV typically shows a less accurate correlation between predicted and identified elastance than the VCV trial. When comparing basis functions, the CUMU basis function set provided the smallest errors overall (median error comparison).

For further comparison, Fig. 7 also shows the 10 % of outliers that were removed displayed in grey. Removal of these points has increased the accuracy of this prediction. In addition, the removal points coincide as 7 %, 20 %, 33 %, and 40 % of outlier points for baseline PEEP = 6, 8, 10 and 12, respectively. This result indicates the outliners leading to less accurate correlation in Fig. 7 are likely due to data quality rather than prediction efficacy of any of the three basis functions.

3.2.2. Peak inspiratory volume (PIV) prediction for PCV

Boxplots of PIV prediction errors (L) across all 4 baseline PEEP prediction groups (baseline PEEP from 6 to 12 cmH_2O) are shown in Fig. 8, while correlations between model predicted PIV and clinical PIV (294 predictions total) are also provided with R^2 values of 0.85, 0.81, and 0.80 for EXP, PARA, and CUMU, respectively. Finally, assessing only clinically relevant ΔPEEP = 2–6 cmH_2O prediction ranges (1 - 3 prediction steps further), Table 4 shows the R^2 values over shorter prediction intervals is higher than the overall values considering all $\Delta PEEP$ levels, ranging from $R^2 = 0.87–0.96$ in the first three rows of the table.

Comparing basis function performance for PCV prediction, the EXP set still yields the overall best performance. Even though EXP and PARA have a similar median error across all 4 prediction groups, CUMU tends to have more outliers and larger IQR, which explains the lower R^2 value.

Table 3
Decreasing R^2 value across different cumulative collections of prediction steps and intervals for all three basis functions for PIP prediction from any baseline $PEEP_1$ level for VCV in the MCREM cohort. The statistics by row are cumulative for 1 step forward, 1 step and 2 steps forward together, up to all 6 steps.

The McREM trial	R^2 value of PIP prediction			Prediction cases
	EXP	PARA	CUMU	
1 step ahead	0.95	0.94	0.96	122
1 and 2 steps ahead	0.95	0.93	0.95	241
1–3 steps ahead	0.93	0.91	0.94	356
1–4 steps ahead	0.92	0.89	0.92	460
1–5 steps ahead	0.91	0.87	0.90	550
1–6 steps ahead	0.90	0.85	0.88	623

3.3. k2end prediction bias: overshoot and undershoot errors

Predictions of PIP and PIV (VCV and PCV respectively) are dependent on the prediction of *k2end*. Prediction of *k2end* is done using the same basis function as applied to the prediction of PIP or PIV. The distension prediction of *k2end* is incorporated to capture any over-distension occurring at the end of inspiration. Thus, this term is directly related to either PIP or PIV, depending on ventilation mode. With overshoot errors, *k2end* was overpredicted, whereas undershoot errors are a result of underpredicted *k2end*. It is important *k2end* is correctly predicted as overdistension results in the over inflation of alveoli and tissue damage, whereas under distension results in lower oxygenation rates and repeated opening and closing of alveoli, or atelectasis.

3.3.1. VCV patients and trial

The boxplots in Fig. 9, show the errors across each of the basis function sets for VCV collated to represent an overall spread and the respective median errors. Fig. 9 shows the boxplots for absolute errors and the signed errors. Overall, the PARA function sets observed the highest absolute median error with a median error of 2.455 cmH_2O, while EXP yields the lowest value of 1.399 cmH_2O. However, as shown in Fig. 9(b), EXP and PARA tend to underestimate and overestimate the PIP predictions, respectively, while the tendency of predictions in CUMU is not obvious.

3.3.2. PCV patients and trial

Boxplots in Fig. 10 depict the signed and absolute errors across each of the basis function sets for PCV, all collated to depict the overall spread and resultant median errors. Unlike the prediction error results for VCV, as shown in Fig. 9, there is no function set that significantly outweighs the performance of the other function sets in PCV. However, the absolute and signed boxplot errors for PIV prediction both agree that the CUMU set observes the highest median prediction error with 0.03 L (absolute) and −0.013 L (signed). Though the signed error is primarily used to show whether a basis function set is overshooting or undershooting, it also shows the true error range where the absolute error range is less functional. The median absolute errors for EXP and PARA are similar, with the PARA set having slightly larger outliers. However, the signed errors show that the PARA set has a larger error range than that of the EXP set. A more obvious representation of this analysis is in Section VCV patients and trial.

4. Discussion

Basis functions have long been proposed to simulate lung mechanics, among other physiological [59–62] and non-physiological system models, as well as in simple to complex lung mechanics models [40,55,56,58,78]. In this approach, three (3) physiologically relevant basis function sets [42,57,63,64] are studied for elastance evolution prediction within the HLM lung mechanics model [42,63] with a goal of assessing overall best performance relative to potential clinical utility. With information identified only from one baseline PEEP level, further prediction of patient-specific lung mechanics response to help optimise MV settings can be accomplished for a targeted higher PEEP level (up to 6 further steps yielding maximum $\Delta PEEP$ = 12 cmH_2O assessed here), without requiring further information.

For PCV, the coupling of tidal volume and flow is the vital problem to conquer for mathematical approaches, where convergence needs to ensure a good balance between model complexity and prediction accuracy. In this approach, the mechanics simulation model is based on [42]. With 3 basis function sets tested, the stability of this nonlinear hysteresis model is further demonstrated in the results presented for both VCV and PCV trials. Further, the ability to accurately predict PIV and PIP provides the ability to safely minimise risk and optimise MV as patient condition evolves.

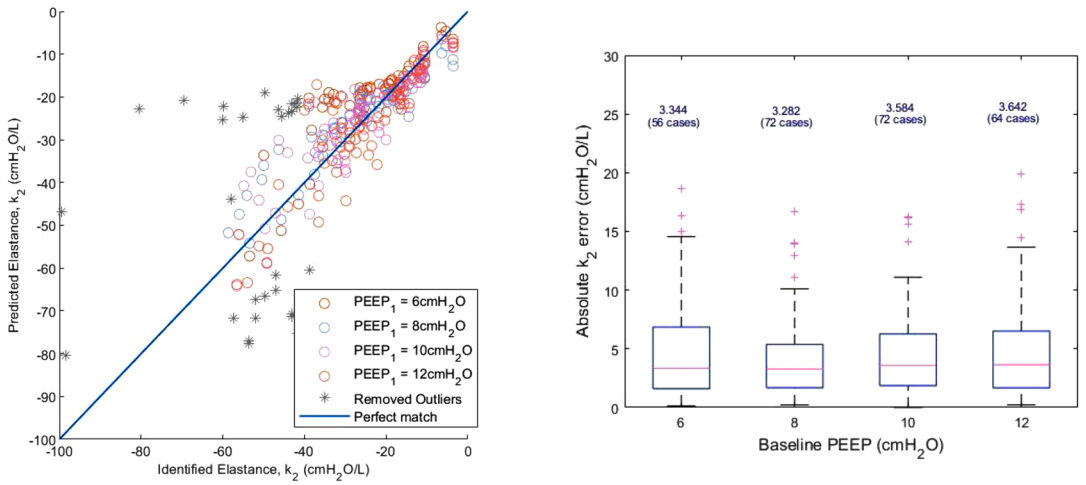

(a) EXP set

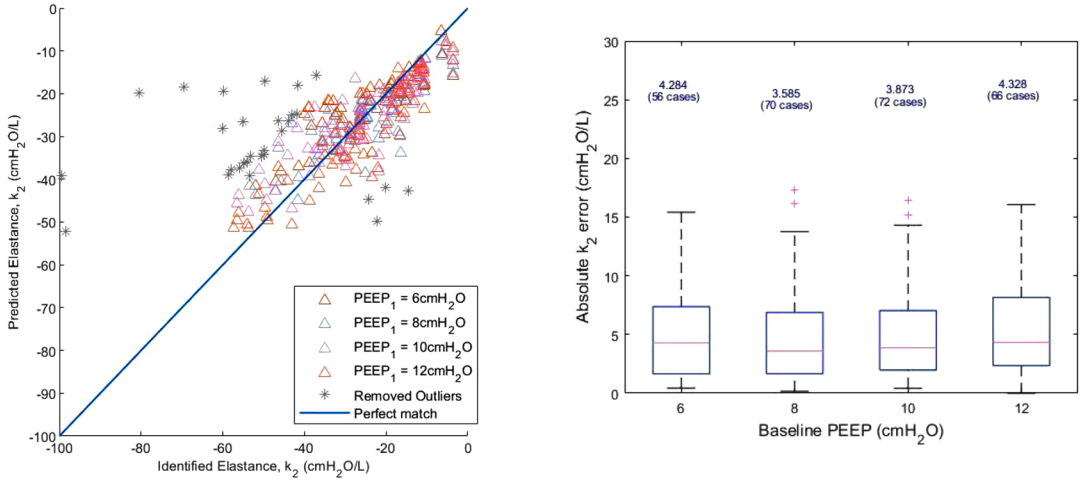

(b) PARA set

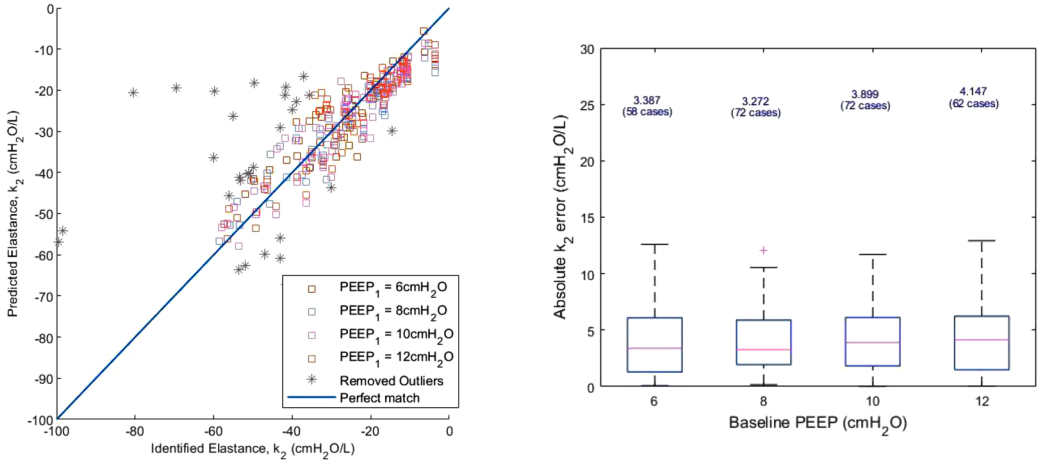

(c) CUMU set

Fig. 7. Correlation plots of Predicted $\mathbf{k}_2$ vs Clinical $\mathbf{k}_2$ (left) and boxplots for $\mathbf{k}_2$ prediction errors with noted median errors (L) over 4 baseline PEEPs (right) for (a) EXP, (b) PARA, and (c) CUMU basis function sets using the PCV MV method.

Correct identification of $k2$ provides a solid base for accurate predictions for PIP/PIV. For the VCV trial, as shown in Fig. 5, there is a clear trend across all three basis functions where the identified $k2$ value is typically higher than predicted. This bias result matches Fig. 9(b) where overshoots are observed across all three basis functions for VCV. Amongst these three basis functions, the CUMU set observed the highest average median error of 5.622 cmH_2O. These averages are derived from the seven median absolute errors at each baseline PEEP level. In

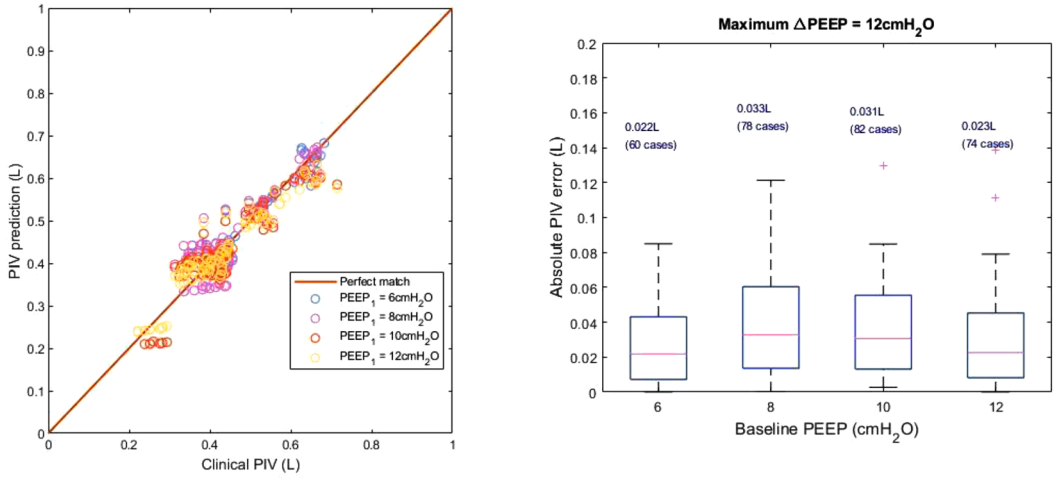

(a) EXP set

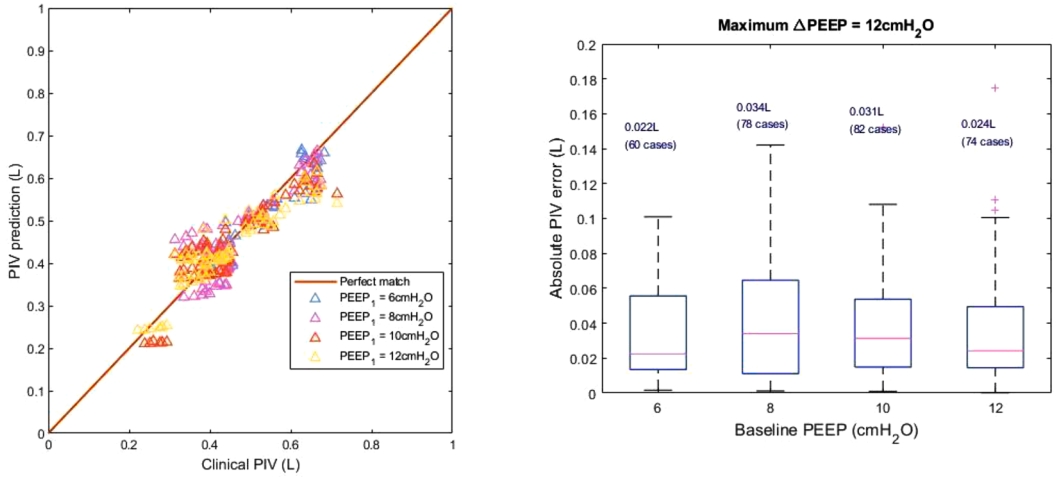

(b) PARA set

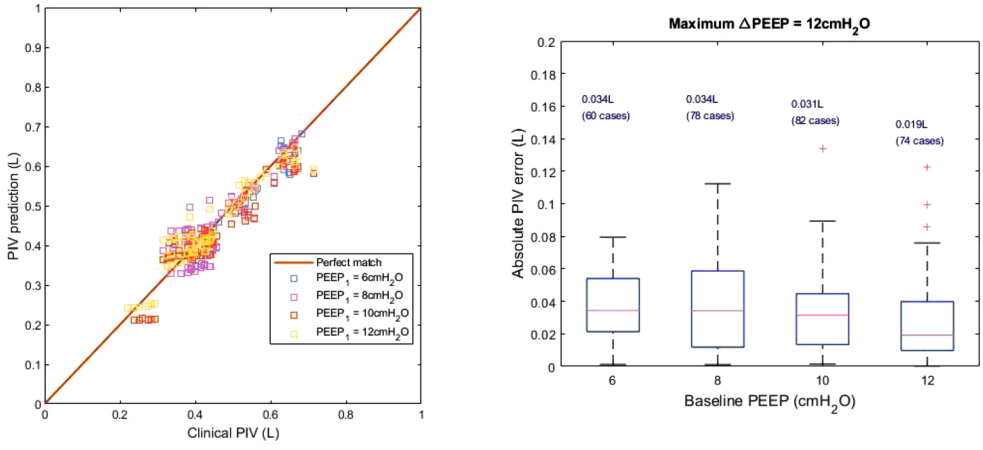

(c) CUMU set

Fig. 8. Correlation plots of Predicted PIV vs Clinical PIV (left) and boxplots for PIV prediction errors with noted median errors (L) over 4 baseline PEEPs (right) for (a) EXP, (b) PARA, and (c) CUMU basis function sets, yielding overall $R^2 = 0.85$ in EXP, $R^2 = 0.81$ in PARA, and $R^2 = 0.80$ in CUMU among 294 prediction cases in PCV.

predicted PIP, which is 50.2 % greater than the lowest average median error of 2.798 cmH_2O associated with the PARA set. The EXP set yielded an average median error of 3.744 cmH_2O. For the PCV trial, as shown in *Fig. 7*, the data is spread more evenly around the 'perfect match' 1:1 line indicating that both overshoot and undershoot are observed more evenly compared to the VCV trial. However, identified $k2$ is still

Table 4
Decreasing R^2 value across different cumulative collections of prediction steps intervals for all three basis function shapes for PIV prediction from any baseline $PEEP_1$ level for PCV in the Maastricht cohort. The statistics by row are cumulative for 1 step forward, 1 step and 2 steps forward together, up to all 4 steps forward for the whole cohort. Thus, the last row presents the total cohort values.

Maastricht	R^2 value of PIV prediction			Prediction cases
	EXP	PARA	CUMU	
1 step further	0.96	0.95	0.96	51
2 step further	0.94	0.90	0.92	102
3 step further	0.91	0.87	0.88	153
4 step further	0.88	0.84	0.84	204
5 step further	0.87	0.82	0.82	253
6 step further	0.85	0.81	0.80	294

typically higher than the predicted. Across the three basis functions, the PARA set had the highest average median error across all baseline PEEP levels of 4.328 cmH_2O (derived from each median absolute error individually) which was 24.4 % higher than the lowest average median error of 3.272 cmH_2O associated with the CUMU set. The EXP set yielded an average median $k2$ prediction error in PCV of 3.463 cmH_2O.

For the VCV trial, as shown in Table 3 the PARA set yields the lowest overall R^2 value, $R^2 = 0.85$, among 623 prediction cases totally. This result occurs due to 70.6 % of predictions overshooting the data for 440 out of 623 cases, compared with 60.8 % and 50.3 % for EXP and CUMU, while some positive bias can lead to a more conservative clinical decision. As shown in Figure 6EXP has a more robust and accurate prediction than CUMU, with lower IQR upper limit PIP prediction error and fewer outliers. Note at lower baseline PEEP values (0 - 4 cmH_2O), although CUMU has a relatively lower median error, it has more outliers and larger IQR compared with the EXP results.

The overall absolute median error for PIP prediction in Fig. 6 tends to decrease as baseline PEEP increases. This outcome is possibly a result of slightly fewer prediction cases as baseline PEEP increases. However, given the relatively large number of predictions, the lower error at clinically relevant PEEP levels and clinically relevant smaller changes in PEEP is important. Equally, the higher prediction errors at lower baseline PEEP, from 0 to 4 cmH_2O, are relatively less critical and harmful for patients compared with higher baseline PEEP, where higher PIP and higher PIP prediction errors increases risk of VILI [13,79]. Similarly,

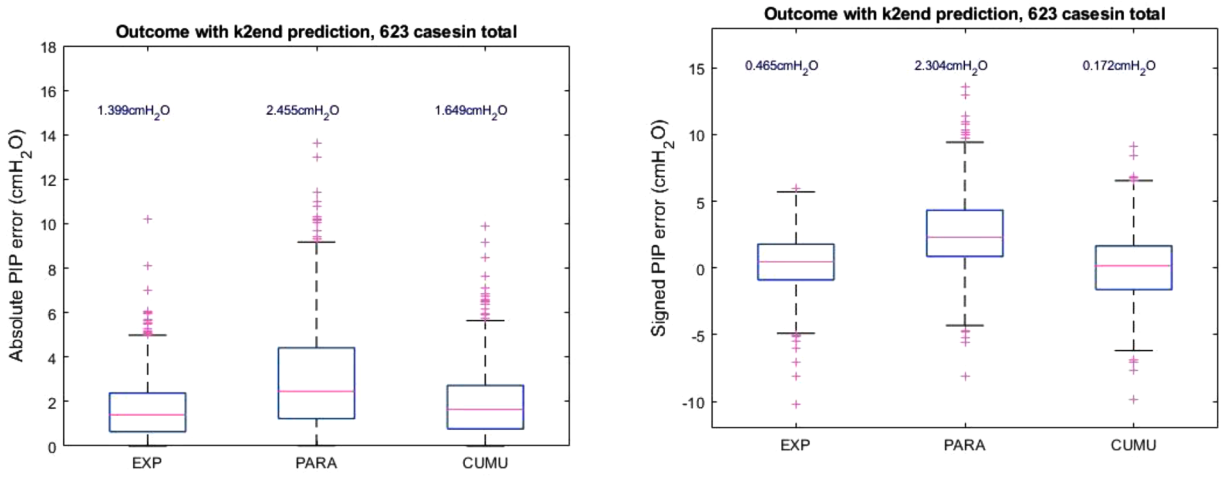

(a) Absolute errors with $k2end$ prediction (b) Signed errors with $k2end$ prediction

Fig. 9. Comparison of absolute PIP prediction errors across 3 basis function sets (a) and (b) with signed prediction errors for the VCV data set (McREM).

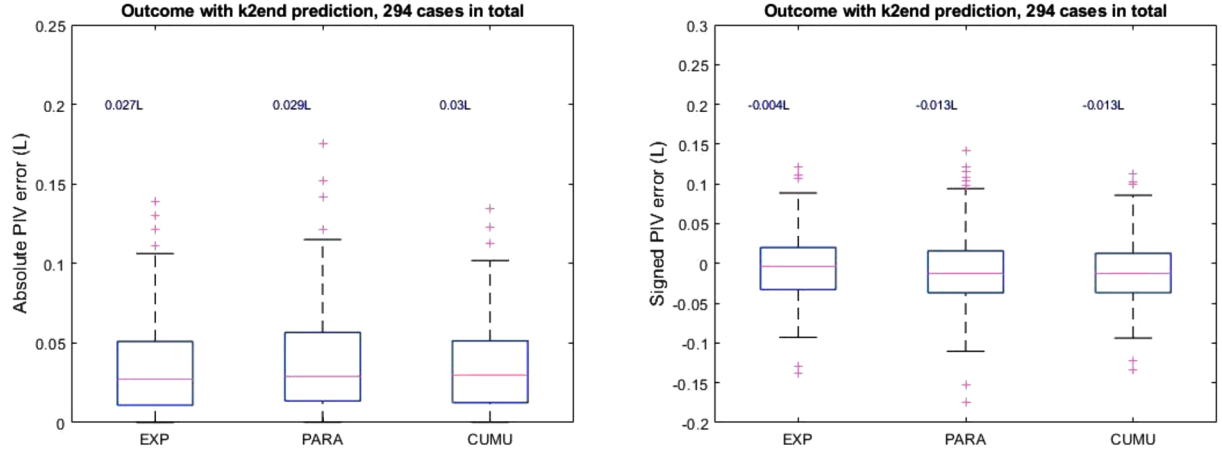

(a) Absolute errors with $k2end$ prediction (b) Signed errors with $k2end$ prediction

Fig. 10. Comparison of absolute PIV prediction errors across 3 basis function sets (a) and (b) with signed prediction errors for the PCV data set (Maastricht).

such low baseline PEEP levels are rarely encountered in adult ICU patients, as such low levels of MV support are supplied by less invasive or controlled ventilation modes [13,80], for which similar virtual patients are being derived [81,82].

For the VCV trial, the overall absolute and signed errors were analysed for PIP in Fig. 9. The signed median errors show that all three function sets observe an overall overshoot in the predicted PIP, the maximum signed median error being the PARA set at 2.304 cmH_2O and lowest signed median error being the CUMU set at 0.172 cmH_2O. The CUMU set also has the largest error spread with outliers at both overshoot and undershoot ends. The outliers for the PARA set are primarily within the overshoot region, whereas EXP set errors are primarily within the undershoot region. Considering the boxplots in Fig. 10 and the disparities between each function set, signed and absolute, the EXP function set yields the most consistent and accurate data for the predictions of PIP. Though it didn't yield the lowest signed median PIP error, the spread of this data and median results from the other analyses all coincide to agree with the verdict that EXP is best function set for these predictions.

Prediction of PIP is also largely based off elastance predictions. Section 3.1.1 highlights an overall undershoot in the prediction of elastance across all three basis functions. However, an overall overshoot was observed in the prediction of PIP. Conversely, Section 3.2.1 shows an overall overshoot in the elastance prediction in PCV where the PIV prediction undershoots oppositely. The way the models have adjusted to overshoot or undershoot correspondingly hints at the possibility of model compensation, such that where the elastance undershoots, the PIP will overshoot to provide a more balanced overall model.

The overall absolute and signed errors were also analysed for the PCV trial in Fig. 10. Signed errors for PIV analysis across the three basis function sets all show an undershoot in their predictions. The maximum signed median PIV error being −0.013 L from both the CUMU and PARA function sets. This is consistent with the two higher absolute median PIV errors corresponding to the CUMU and PARA sets. The highest absolute median PIV error being 0.03 L from the CUMU function set. The lowest signed median PIV error being 0.04 L and the lowest absolute median PIV error being 0.027 L, both from the EXP function set. In both sets, the PARA set observed the largest spread, highlighting a larger inconsistency in the results in comparison to the other two function sets. From looking at both the signed and absolute error boxplots in Fig. 10, and considering the differentials between these errors, the EXP set yields the most accurate and stable prediction data for both the PIV predicted data overall.

As for the PARA and CUMU sets, the highest errors occur somewhat randomly. Thus, the EXP set yields the most stable and accurate prediction across different baseline PEEP levels for VCV. All these results are consistent with reduced errors when considering only the first, clinically relevant 2–3 PEEP steps. This choice reflects balancing trade-offs between accuracy and robustness.

Similarly, higher median PIV prediction errors in PCV patients occur where there are more baseline PEEP prediction cases. The EXP set still yields the best prediction performance across various baseline PEEP levels, while 90 % of PIV errors are within 0.068 L, compared with 0.077 L and 0.078 L in PARA and CUMU sets respectively. Moreover, the median PIV error decreases to 0.019 L from 0.028 L while all errors are within 0.079 L for EXP if the maximum $\Delta PEEP$ for prediction narrows to 6 cmH_2O (3 prediction steps) from 12 cmH_2O (6 prediction steps), which is a more clinically realistic setting. In these clinically realistic cases, the R^2 values increase, with similar improvement in VCV predictions, as shown in Table 4.

For PCV prediction, the CUMU set has the lowest R^2 value, $R^2 = 0.80$, with 90 % of PIV prediction errors within 0.078 L. In EXP and PARA, 90 % of errors are lower than 0.068 L and 0.077 L, respectively. As shown in Fig. 8, comparing performance between EXP and CUMU sets, the latter has lower median PIV error, but more and larger outliers. Overall, the EXP set yields to the most robust prediction over all 3 basis function sets.

Knowing a patients optimal elastance and recruitable volume allows clinicians to select an appropriate PEEP for optimal ventilation. Prediction models and algorithms would enable these clinicians with an assistive tool to indicate what the optimal ventilation settings are for that patient specifically by using patient-specific prediction models. Having the correct ventilator settings will minimise the likelihood of overdistension occurring and in turn minimise the occurrence of VILI in patients post ventilator therapy.

The efficacy of $k2end$ is validated with prior work [72]. It is kept the same in this study across all three basis functions to predict the over-distension at higher PEEP levels. The PIP and PIV predictions bias and errors are possibly affected by both the applied basis function set and k2end function. However, the elastance predictions at lower baseline PEEP levels shown in Figs. 5 and 7, where over-distension is rarely seen, present the difference across basis function sets.

This model will be run through multiple different data sets before conclusively stating its complete ability. After using data sets McREM and Maastricht, the predictive model is showing large promise. Accuracy of the predictive software when looking at PIV (PCV), PIP (VCV) and $k2$ is high, particularly for VCV mode (approx. 96 %). However, alterations to improve the accuracy of predictions to the PCV mode model are required and underway.

While predictive models have been increasingly developed and tested, integrating the proposed predictive model in the clinical control loop remains a challenge because the practical implementation of the proposed model in real patients would require rigorous clinical trials and assessment to ensure its robustness and safety [28,29,83,84]. In addition, engagement of clinical staff would still be required to ensure the oversight, planning and safety of the intervention. Therefore, beyond the technology factors, social factors should also be considered for appropriate change management processes in addition to workload management to enable appropriate levels of engagement with technology and training prior to the model use in real world.

In this work we have analysed three potential basis functions. These were chosen based off physiological compatibility and previous work within the same framework. However, this work does not preclude better basis functions or a different hysteretic model with different or similar basis functions from performing better.

In summary, the EXP set yields the best performance across various baseline PEEP levels and MV modes, VCV and PCV. Although the PARA and CUMU sets are not as good as the EXP set overall, they do show very promising ability, and might be further optimised. Overall, the results show the potential power of personalised models to predict outcomes to changes in care using physiologically relevant basis function sets. Model-based approaches to personalising care require far less added hardware, added data, or/and personnel costs, and require only relatively limited computation as found on bedside computers or cloud served computation. Moreover, the 3 basis function sets examined in this approach can still be improved with further tests and offer new insights for researchers to study and consider the inner correlation between elastance prediction and respiratory response prediction for model optimizing.

5. Conclusion

This study presents the prediction performance of 3 physiologically relevant basis function sets across 32 ventilated patients (18 VCV, 14 PCV) at a wide range of different baseline PEEP levels with $\Delta PEEP$ prediction intervals up to 12 cmH_2O. While all 3 sets yield very good predictions for both VCV and PCV, the exponential basis function set, EXP, has the best performance across both PCV and VCV modes, and the most robust prediction performance in both modes, thus providing a best balance of accuracy and robustness. The overall outcome shows all three physiologically relevant basis function sets offer the possibility for accurate and simpler lung mechanics prediction, and how otherwise similar basis function forms can lead to different prediction outcomes for

both elastance and pulmonary response. This latter outcome indicates the need to test robustness over basis function shapes when using this approach for any type of digital twin or virtual patient model, which has not been tested previously. Thus, the main results offer new insights into how to consider and optimize lung mechanics models with elastance evolution function forms for further studies, and the basis function shapes themselves create new potential hypotheses to better understanding the macro behaviour of lung tissue mechanics in mechanical ventilation.

Declaration of Competing Interest

The authors on this submission declare that there are no conflicts of interest on this paper, financial or otherwise.

Acknowledgements

This work was supported by the NZ Tertiary Education Commission (TEC) fund MedTech CoRE (Centre of Research Excellence; #3705718), the NZ National Science Challenge 7, Science for Technology and Innovation (2019-S3-CRS) and the Nature Science Foundation of China (NSFC) Grant No 12102362. The authors also acknowledge support from the EU H2020 R&I programme (MSCA-RISE-2019 call) under grant agreement #872488 — DCPM, and a University of Canterbury Doctoral Scholarship.

Supplementary materials

Supplementary material associated with this article can be found, in the online version, at doi:10.1016/j.cmpb.2023.107988.

References

[1] M.B.P. Amato, C.S.V. Barbas, D.M. Medeiros, R.B. Magaldi, G.P. Schettino, G. Lorenzi-Filho, R.A. Kairalla, D. Deheinzelin, C. Munoz, R. Oliveira, T. Y. Takagaki, C.R.R. Carvalho, Effect of a protective-ventilation strategy on mortality in the acute respiratory distress syndrome, N. Engl. J. Med. 338 (6) (1998) 347–354.

[2] P. Severgnini, G. Selmo, C. Lanza, A. Chiesa, A. Frigerio, A. Bacuzzi, G. Dionigi, R. Novario, C. Gregoretti, M.G. de Abreu, M.J. Schultz, S. Jaber, E. Futier, M. Chiaranda, P. Pelosi, Protective mechanical ventilation during general anesthesia for open abdominal surgery improves postoperative pulmonary function, Anesthesiology: J. Am. Soc. Anesthesiol. 118 (6) (2013) 1307–1321.

[3] D.M. Needham, E. Colantuoni, P.A. Mendez-Tellez, V.D. Dinglas, J.E. Sevransky, C. R. Dennison Himmelfarb, S.V. Desai, C. Shanholtz, R.G. Brower, P.J. Pronovost, Lung protective mechanical ventilation and two year survival in patients with acute lung injury: prospective cohort study, BMJ: Br. Med. J. 344 (2012) e2124.

[4] A. Paternot, X. Repessé, A. Vieillard-Baron, Rationale and description of right ventricle-protective ventilation in ARDS, Respir. Care 61 (10) (2016) 1391–1396.

[5] E. Marret, R. Cinotti, L. Berard, V. Piriou, J. Jobard, B. Barrucand, D. Radu, S. Jaber, F. Bonnet, group, a.t.P.s., 'Protective ventilation during anaesthesia reduces major postoperative complications after lung cancer surgery: a double-blind randomised controlled trial, Eur. J. Anaesthesiol. | EJA 35 (10) (2018) 727–735.

[6] M.O. Meade, D.J. Cook, G.H. Guyatt, A.S. Slutsky, Y.M. Arabi, D.J. Cooper, A. R. Davies, L.E. Hand, Q. Zhou, L. Thabane, P. Austin, S. Lapinsky, A. Baxter, J. Russell, Y. Skrobik, J.J. Ronco, T.E. Stewart, Lung Open Ventilation Study Investigators, f.t., Ventilation strategy using low tidal volumes, recruitment maneuvers, and high positive end-expiratory pressure for acute lung injury and acute respiratory distress syndrome: a randomized controlled trial, JAMA 299 (6) (2008) 637–645.

[7] M.B.P. Amato, M.O. Meade, A.S. Slutsky, L. Brochard, E.L.V. Costa, D. A. Schoenfeld, T.E. Stewart, M. Briel, D. Talmor, A. Mercat, J.-C.M. Richard, C.R. R. Carvalho, R.G. Brower, Driving pressure and survival in the acute respiratory distress syndrome, N. Engl. J. Med. 372 (8) (2015) 747–755.

[8] J. Nakahira, S. Nakano, T. Minami, 'Evaluation of alveolar recruitment maneuver on respiratory resistance during general anesthesia: a prospective observational study, BMC Anesthesiol. 20 (1) (2020) 264.

[9] G.H. Fodor, S. Bayat, G. Albu, N. Lin, A. Baudat, J. Danis, F. Peták, W. Habre, Variable ventilation is equally effective as conventional pressure control ventilation for optimizing lung function in a rabbit model of ARDS, Front. Physiol. 10 (803) (2019).

[10] O. Writing Group for the Alveolar Recruitment for Acute Respiratory Distress Syndrome Trial, I. Cavalcanti, A.B. Suzumura, É.A. Laranjeira, L.N. Paisani, D.d. M. Damiani, L.P. Guimarães, H.P. Romano, E.R. Regenga, M.d.M. Taniguchi, L.N. T. Teixeira, C. Pinheiro de Oliveira, R. Machado, F.R. Diaz-Quijano, F.A. Filho, M.S. d.A. Maia, I.S. Caser, E.B. Filho, W.d.O. Borges, M.d.C. Martins, P.d.A. Matsui, M. Ospina-Tascón, G.A. Giancursi, T.S. Giraldo-Ramirez, N.D. Vieira, S.R.R. Assef, M.d.G.P.d.L. Hasan, M.S. Szczeklik, W. Rios, F. Amato, M.B.P. Berwanger, C. R. Ribeiro de Carvalho, Effect of lung recruitment and titrated positive end-expiratory pressure (PEEP) vs low PEEP on mortality in patients with acute respiratory distress syndrome: A Randomized Clinical Trial JAMA, 318 (14) (2017) 1335–1345.

[11] M. Pirrone, D. Fisher, D. Chipman, D.A.E. Imber, J. Corona, C. Mietto, R. M. Kacmarek, L. Berra, Recruitment maneuvers and positive end-expiratory pressure titration in morbidly obese ICU patients, Crit. Care Med. 44 (2) (2016) 300–307.

[12] B. O'Gara, D. Talmor, 'Perioperative lung protective ventilation, BMJ 362 (2018) k3030.

[13] V.J. Major, Y.S. Chiew, G.M. Shaw, J.G. Chase, Biomedical engineer's guide to the clinical aspects of intensive care mechanical ventilation, Biomed. Eng. Online 17 (1) (2018) 169.

[14] D. Carney, J. DiRocco, G. Nieman, Dynamic alveolar mechanics and ventilator-induced lung injury, Crit. Care Med. 33 (3) (2005) S122–S128.

[15] L. Pavone, S. Albert, J. DiRocco, L. Gatto, G. Nieman, Alveolar instability caused by mechanical ventilation initially damages the nondependent normal lung, Crit. Care 11 (5) (2007) R104.

[16] J.D. Ricard, D. Dreyfuss, G. Saumon, Ventilator-induced lung injury, Eur. Respir. J. 22 (42_suppl) (2003), 2s-9.

[17] M.D. Zilberberg, S.K. Epstein, Acute lung injury in the medical ICU. Comorbid conditions, age, etiology, and hospital outcome, Am. J. Respir. Crit. Care Med. 157 (4) (1998) 1159–1164.

[18] D. Dreyfuss, G. Saumon, Ventilator-induced lung injury. Lessons from experimental studies, Am. J. Respir. Crit. Care Med. 157 (1) (1998) 294–323.

[19] V.M. Ranieri, P.M. Suter, C. Tortorella, R. De Tullio, J.M. Dayer, A. Brienza, F. Bruno, A.S. Slutsky, Effect of mechanical ventilation on inflammatory mediators in patients with acute respiratory distress syndrome: a randomized controlled trial, JAMA 282 (1999) 54–61.

[20] A.B. Adams, D.A. Simonson, D.J. Dries, Ventilatory-induced lung injury, Respir. Care Clin. N. Am. 9 (3) (2003) 343–362.

[21] B. O. Gajic, S.I. Dara, J.L. Mendez, A.O. Adesanya, E. Festic, S.M. Caples, R. Rana, St. Sauver, J.L. Lymp, J.F. Afessa, R.D. Hubmayr, Ventilator-associated lung injury in patients without acute lung injury at the onset of mechanical ventilation Crit. Care Med. 32 (9) (2004) 1817–1824.

[22] E.D. Moloney, M.J.D. Griffiths, Protective ventilation of patients with acute respiratory distress syndrome, Br. J. Anaesth. 92 (2) (2004) 261–270.

[23] P.E. Parsons, M.D. Eisner, B.T. Thompson, M.A. Matthay, M. Ancukiewicz, G. R. Bernard, A.P. Wheeler, Network, t.N.A.R.D.S.C.T., 'Lower tidal volume ventilation and plasma cytokine markers of inflammation in patients with acute lung injury, Crit. Care Med. 33 (1) (2005) 1–6.

[24] J. Villar, Ventilator or physician-induced lung injury? Minerva Anestesiol. 71 (6) (2005) 255–258.

[25] B. Lobo, C. Hermosa, A. Abella, F. Gordo, Electrical impedance tomography, Ann. Transl. Med. 6 (2) (2018) 26.

[26] S.E. Morton, J.L. Knopp, J.G. Chase, K. Möller, P. Docherty, G.M. Shaw, M. Tawhai, Predictive virtual patient modelling of mechanical ventilation: impact of recruitment function, Ann. Biomed. Eng. 47 (7) (2019) 1626–1641.

[27] M. Laviola, D.G. Bates, J.G. Hardman, Mathematical and computational modelling in critical illness, Eur. Respir. Pulm. Dis. 5 (1) (2019).

[28] J.G. Chase, J.-C. Preiser, J.L. Dickson, A. Pironet, Y.S. Chiew, C.G. Pretty, G. M. Shaw, B. Benyo, K. Moeller, S. Safaei, M. Tawhai, P. Hunter, T. Desaive, Next-generation, personalised, model-based critical care medicine: a state-of-the art review of in silico virtual patient models, methods, and cohorts, and how to validation them, Biomed. Eng. Online 17 (1) (2018) 24.

[29] Geoffrey Chase, J.; Zhou, C.; Knopp, J.L.; Moeller, K.; Benyo, B.; Xe, Z.S.; Desaive, T.; Wong, J.H.K.; Malinen, S.; Naswall, K.; Shaw, G.M.; Lambermont, B.; Chiew, Y. S., 'Digital twins and automation of care in the intensive care unit' (2023).

[30] K.T. Kim, S. Morton, S. Howe, Y.S. Chiew, J.L. Knopp, P. Docherty, C. Pretty, T. Desaive, B. Benyo, A. Szlavecz, Model-based PEEP titration versus standard practice in mechanical ventilation: a randomised controlled trial, Trials 21 (1) (2020) 130.

[31] Y.S. Chiew, J.G. Chase, G.M. Shaw, A. Sundaresan, T. Desaive, 'Model-based PEEP optimisation in mechanical ventilation, Biomed. Eng. Online 10 (1) (2011) 111.

[32] K.G. Hickling, The pressure–volume curve is greatly modified by recruitment, Am. J. Respir. Crit. Care Med. 158 (1) (1998) 194–202.

[33] M. Briel, M. Meade, A. Mercat, R.G. Brower, D. Talmor, S.D. Walter, A.S. Slutsky, E. Pullenayegum, Q. Zhou, D. Cook, L. Brochard, J.-C.M. Richard, F. Lamontagne, N. Bhatnagar, T.E. Stewart, G. Guyatt, Higher vs lower positive end-expiratory pressure in patients with acute lung injury and acute respiratory distress syndrome: systematic review and meta-analysis, JAMA 303 (9) (2010) 865–873.

[34] A. Sundaresan, J.G. Chase, G.M. Shaw, Y.S. Chiew, T. Desaive, Model-based optimal PEEP in mechanically ventilated ARDS patients in the Intensive Care Unit, Biomed. Eng. Online 10 (1) (2011) 64.

[35] N.S. Damanhuri, Y.S. Chiew, N.A. Othman, P.D. Docherty, C.G. Pretty, G.M. Shaw, T. Desaive, J.G. Chase, Assessing respiratory mechanics using pressure reconstruction method in mechanically ventilated spontaneous breathing patient, Comput. Methods Programs Biomed. 130 (2016) 175–185.

[36] A. Sundaresan, J.G. Chase, Positive end expiratory pressure in patients with acute respiratory distress syndrome – The past, present and future', Biomed. Signal Process. Control 7 (2) (2012) 93–103.

[37] C.B. Massa, G.B. Allen, J.H.T. Bates, Modeling the dynamics of recruitment and derecruitment in mice with acute lung injury, J. Appl. Physiol. 105 (6) (2008) 1813–1821.
[38] K.L. Steimle, M.L. Mogensen, D.S. Karbing, J. Bernardino de la Serna, S. Andreassen, A model of ventilation of the healthy human lung, Comput. Methods Programs Biomed. 101 (2) (2011) 144–155.
[39] Y.S. Chiew, J.G. Chase, B. Lambermont, N. Janssen, C. Schranz, K. Moeller, G. M. Shaw, T. Desaive, Physiological relevance and performance of a minimal lung model – an experimental study in healthy and acute respiratory distress syndrome model piglets, BMC Pulm. Med. 12 (1) (2012) 59.
[40] S.E. Morton, J.L. Knopp, J.G. Chase, P. Docherty, S.L. Howe, K. Möller, G.M. Shaw, M. Tawhai, Optimising mechanical ventilation through model-based methods and automation, Annu. Rev. Control 48 (2019) 369–382.
[41] S.E. Morton, J.L. Knopp, M.H. Tawhai, P. Docherty, S.J. Heines, D.C. Bergmans, K. Möller, J.G. Chase, Prediction of lung mechanics throughout recruitment maneuvers in pressure-controlled ventilation, Comput. Methods Programs Biomed. 197 (2020), 105696.
[42] C. Zhou, J.G. Chase, J. Knopp, Q. Sun, M. Tawhai, K. Möller, S.J. Heines, D. C. Bergmans, G.M. Shaw, T. Desaive, 'Virtual patients for mechanical ventilation in the intensive care unit, Comput. Methods Programs Biomed. 199 (2021), 105912.
[43] B.D. Singer, T.C. Corbridge, Pressure modes of invasive mechanical ventilation, South Med. J. 104 (10) (2011) 701–709.
[44] L. Ashworth, Y. Norisue, M. Koster, J. Anderson, J. Takada, H. Ebisu, Clinical management of pressure control ventilation: an algorithmic method of patient ventilatory management to address "forgotten but important variables, J. Crit. Care 43 (2018) 169–182.
[45] O. Sen, M. Bakan, T. Umutoglu, N. Aydın, M. Toptas, I. Akkoc, Effects of pressure-controlled and volume-controlled ventilation on respiratory mechanics and systemic stress response during prone position, Springerplus 1 (5) (2016) 1761.
[46] P. Cadi, T. Guenoun, D. Journois, J.-M. Chevallier, J.-L. Diehl, D. Safran, Pressure-controlled ventilation improves oxygenation during laparoscopic obesity surgery compared with volume-controlled ventilation, BJA: Br. J. Anaesth. 100 (5) (2008) 709–716.
[47] D. Nichols, S. Haranath, Pressure control ventilation, Crit. Care Clin. 23 (2) (2007) 183–199.
[48] R.S. Campbell, B.R. Davis, Pressure-controlled versus volume-controlled ventilation: does it matter? Respir. Care 47 (4) (2002) 416–424, discussion 424-416.
[49] L. Ball, M. Dameri, P. Pelosi, Modes of mechanical ventilation for the operating room, Best Pract. Res. Clin. Anaesth. 29 (3) (2015) 285–299.
[50] T. Tonetti, F. Vasques, F. Rapetti, G. Maiolo, F. Collino, F. Romitti, L. Camporota, M. Cressoni, P. Cadringher, M. Quintel, L. Gattinoni, Driving pressure and mechanical power: new targets for VILI prevention, Ann. Transl. Med. 5 (14) (2017) 286.
[51] A.J. Garnero, H. Abbona, F. Gordo-Vidal, C. Hermosa-Gelbard, Pressure versus volume controlled modes in invasive mechanical ventilation, Med. Intensiva (Eng. Ed.) 37 (4) (2013) 292–298.
[52] M. Keszler, Volume-targeted ventilation, Early Hum. Dev. 82 (12) (2006) 811–818.
[53] N. Rittayamai, C.M. Katsios, F. Beloncle, J.O. Friedrich, J. Mancebo, L. Brochard, Pressure-Controlled vs Volume-Controlled ventilation in acute respiratory failure: a physiology-based narrative and systematic review, Chest 148 (2) (2015) 340–355.
[54] K.L. Hamlington, B.J. Smith, G.B. Allen, J.H. Bates, Predicting ventilator-induced lung injury using a lung injury cost function, J. Appl. Physiol. (Bethesda, Md.: 1985) 121 (1) (2016) 106–114.
[55] B. Laufer, P.D. Docherty, A. Knörzer, Y.S. Chiew, R. Langdon, K. Möller, J.G. Chase, Performance of variations of the dynamic elastance model in lung mechanics, Control Eng. Pract. 58 (2017) 262–267.
[56] Kanae, S.; Muramatsu, K.; Yang, Z.J.; and Wada, K., 'Modeling of respiration and estimation of pulmonary elastance', in: 'Book Modeling of Respiration and Estimation of Pulmonary Elastance' 641(2004)649–652.
[57] S.E. Morton, J. Dickson, J.G. Chase, P. Docherty, T. Desaive, S.L. Howe, G.M. Shaw, M. Tawhai, A virtual patient model for mechanical ventilation, Comput. Methods Programs Biomed. 165 (2018) 77–87.
[58] R. Langdon, P.D. Docherty, Y.S. Chiew, J.G. Chase, Extrapolation of a non-linear autoregressive model of pulmonary mechanics, Math. Biosci. 284 (2017) 32–39.
[59] R. Langdon, P.D. Docherty, E.J. Mansell, J.G. Chase, Accurate and precise prediction of insulin sensitivity variance in critically ill patients, Biomed. Signal Process. Control 39 (2018) 327–335.
[60] K.W. Stewart, C.G. Pretty, G.M. Shaw, J.G. Chase, Creating smooth SI. B-spline basis function representations of insulin sensitivity, Biomed. Signal Process. Control 44 (2018) 270–278.
[61] A. Gani, A.V. Gribok, S. Rajaraman, W.K. Ward, J. Reifman, Predicting subcutaneous glucose concentration in humans: data-driven glucose modeling, IEEE Trans. Biomed. Eng. 56 (2) (2008) 246–254.
[62] M.P. Reymann, E. Dorschky, B.H. Groh, C. Martindale, P. Blank, B.M. Eskofier, Blood glucose level prediction based on support vector regression using mobile platforms, in Editor (Ed.)^(Eds.). Book Blood Glucose Level Prediction Based On Support Vector Regression Using Mobile Platforms, IEEE, 2016, pp. 2990–2993. edn.
[63] C. Zhou, J.G. Chase, Q. Sun, J. Knopp, A nonlinear hysteretic model for automated prediction of lung mechanics during mechanical ventilation, in: IFAC-PapersOnLine 53, 2020, pp. 817–822.
[64] Sun, Q.; Chase, J.G.; Zhou, C.; Tawhai, M.H.; Knopp, J.L.; Möller, K.; Heines, S.J.; Bergmans, D.C.; and Shaw, G.M., 'Simplified basis-function-based virtual patient model in lung mechanics prediction under mechanical ventilation', Biological and Medical Systems - 11th BMS 2021, In press.
[65] D. Dreyfuss, G. Saumon, Role of tidal volume, FRC, and end-inspiratory volume in the development of pulmonary Edema following mechanical ventilation, Am. Rev. Respir. Dis. 148 (5) (1993) 1194–1203.
[66] r J.J. Marini, P.S. Crooke, J.D. Truwit, Determinants and limits of pressure-preset ventilation: a mathematical model of pressure control, J. Appl. Physiol. 67 (3) (1989) 1081–1092.
[67] A.B. Adams, N. Cakar, J.J. Marini, Static and dynamic pressure-volume curves reflect different aspects of respiratory system mechanics in experimental acute respiratory distress syndrome, Respir. Care 46 (7) (2001) 686–693.
[68] M. Tang, W. Wang, J. Wheeler, M. McCormick, X. Dong, 'The number of electrodes and basis functions in EIT image reconstruction, Physiol. Meas. 23 (1) (2002) 129.
[69] K.W. Stewart, C.G. Pretty, G.M. Shaw, J.G. Chase, Interpretation of retrospective BG measurements, J. Diabetes Sci. Technol. 12 (5) (2018) 967–975.
[70] R. Langdon, P.D. Docherty, C. Schranz, J.G. Chase, Prediction of high airway pressure using a non-linear autoregressive model of pulmonary mechanics, Biomed. Eng. Online 16 (1) (2017) 126.
[71] Q. Sun, C. Zhou, J.G. Chase, Parameter updating of a patient-specific lung mechanics model for optimising mechanical ventilation, Biomed. Signal Process. Control 60 (2020), 102003.
[72] Q. Sun, J.G. Chase, C. Zhou, M.H. Tawhai, J.L. Knopp, K. Möller, G.M. Shaw, Over-distension prediction via hysteresis loop analysis and patient-specific basis functions in a virtual patient model, Comput. Biol. Med. 141 (2021), 105022.
[73] Q. Sun, J.G. Chase, C. Zhou, M.H. Tawhai, J.L. Knopp, K. Möller, S.J. Heines, D. C. Bergmans, G.M. Shaw, Prediction and estimation of pulmonary response and elastance evolution for volume-controlled and pressure-controlled ventilation, Biomed. Signal Process. Control 72 (2022), 103367.
[74] Q. Sun, J.G. Chase, C. Zhou, M.H. Tawhai, J.L. Knopp, K. Möller, G.M. Shaw, Over-distension prediction via hysteresis loop analysis and patient-specific basis functions in a virtual patient model, Comput. Biol. Med. 141 (2022), 105022.
[75] E.C. Goligher, E.L.V. Costa, C.J. Yarnell, L.J. Brochard, T.E. Stewart, G. Tomlinson, R.G. Brower, A.S. Slutsky, M.P.B. Amato, Effect of lowering Vt on mortality in acute respiratory distress syndrome varies with respiratory system elastance, Am. J. Respir. Crit. Care Med. 203 (11) (2021) 1378–1385.
[76] C.A. Stahl, K. Möller, S. Schumann, R. Kuhlen, M. Sydow, C. Putensen, J. Guttmann, Dynamic versus static respiratory mechanics in acute lung injury and acute respiratory distress syndrome, Crit. Care Med. 34 (8) (2006) 2090–2098.
[77] M. Sasidhar, R.L. Chatburn, Tidal volume variability during airway pressure release ventilation: case summary and theoretical analysis, Respir. Care 57 (8) (2012) 1325–1333.
[78] G.R. Arunachalam, Y.S. Chiew, C.P. Tan, A.M. Ralib, M.B.M. Nor, Patient asynchrony modelling during controlled mechanical ventilation therapy, Comput. Methods Programs Biomed. (2020) 183.
[79] J.M. Halter, J.M. Steinberg, L.A. Gatto, J.D. DiRocco, L.A. Pavone, H.J. Schiller, S. Albert, H.-M. Lee, D. Carney, G.F. Nieman, Effect of positive end-expiratory pressure and tidal volume on lung injury induced by alveolar instability, Crit. Care 11 (1) (2007) R20.
[80] A. Sundaresan, J.G. Chase, Positive end expiratory pressure in patients with acute respiratory distress syndrome–The past, present and future', Biomed. Signal Process. Control 7 (2) (2012) 93–103.
[81] E.F.S. Guy, J.G. Chase, J.L. Knopp, G.M. Shaw, Quantifying ventilator unloading in CPAP ventilation, Comput. Biol. Med. 142 (2022), 105225.
[82] J.L. Knopp, J.G. Chase, K.T. Kim, G.M. Shaw, Model-based estimation of negative inspiratory driving pressure in patients receiving invasive NAVA mechanical ventilation, Comput. Methods Programs Biomed. 208 (2021), 106300.
[83] D. Eastman, C. McCarthy, Embracing change: healthcare technology in the 21st century, Nurs. Manage. 43 (6) (2012) 52–54.
[84] Kotter, J.P., Leading change: why transformation efforts fail, 2007.